Verification of Single Event Upset Rate Estimation Methods with On-Orbit Observations

Prepared by

M. SHOGA and P. ADAMS
Hughes Aircraft Company
Los Angeles, CA 90007

D. L. CHENETTE and R. KOGA
Space Sciences Laboratory
Laboratory Operations
The Aerospace Corporation
El Segundo, CA 90245

E. C. SMITH
TRW
Redondo Beach, CA 90278

20 June 1988

AD-A196 226

DTIC
SELECTED
JUL 25 1988
H

This report was submitted by The Aerospace Corporation, El Segundo, CA
90245, under Contract No. F04701-85-C-0086 with the Space Division, P.O.
Box 92960, Worldway Postal Center, Los Angeles, CA 90009-2960. It was
reviewed and approved for The Aerospace Corporation by H. R. Rugge,
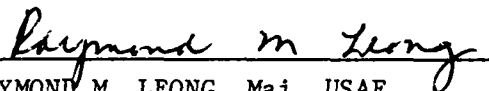Director, Space Sciences Laboratory.

Lt Clarence V. Wilcox was the project officer for the Mission-Oriented
Investigation and Experimentation (MOIE) Program.

This report has been reviewed by the Public Affairs Office (PAS) and
is releasable to the National Technical Information Service (NTIS). At
NTIS, it will be available to the general public, including foreign
nationals.

This technical report has been reviewed and is approved for
publication. Publication of this report does not constitute Air Force
approval of the report's findings or conclusions. It is published only for
the exchange and stimulation of ideas.

CLARENCE V. WILCOX, Lt, USAF
MOIE Project Officer
SD/CLTPC

RAYMOND M. LEONG, Maj, USAF
Deputy Director, AFSTC West Coast Office
AFSTC/WCO OL-AB

REPORT DOCUMENTATION PAGE

1a. REPORT SECURITY CLASSIFICATION Unclassified		1b. RESTRICTIVE MARKINGS
2a. SECURITY CLASSIFICATION AUTHORITY		3. DISTRIBUTION/AVAILABILITY OF REPORT Approved for public release; distribution unlimited.
2b. DECLASSIFICATION/DOWNGRADING SCHEDULE		
4. PERFORMING ORGANIZATION REPORT NUMBER(S) TR-0086A(2940-05)-7		5. MONITORING ORGANIZATION REPORT NUMBER(S) SD-TR-88-68
6a. NAME OF PERFORMING ORGANIZATION The Aerospace Corporation Laboratory Operations	6b. OFFICE SYMBOL (If applicable)	7a. NAME OF MONITORING ORGANIZATION Space Division
6c. ADDRESS (City, State, and ZIP Code) El Segundo, CA 90245		7b. ADDRESS (City, State, and ZIP Code) Los Angeles Air Force Base Los Angeles, CA 90009-2960
8a. NAME OF FUNDING/SPONSORING ORGANIZATION	8b. OFFICE SYMBOL (If applicable)	9. PROCUREMENT INSTRUMENT IDENTIFICATION NUMBER F04701-85-C-0086-P00016

8c. ADDRESS (City, State, and ZIP Code)	10. SOURCE OF FUNDING NUMBERS			
	PROGRAM ELEMENT NO.	PROJECT NO.	TASK NO.	WORK UNIT ACCESSION NO.

11. TITLE (Include Security Classification)

Verification of Single Event Upset Rate Estimation Methods with On-Orbit Observations

12. PERSONAL AUTHOR(S) Shoga, M., Adams, P. (Hughes Aircraft Co.), Chennette, D. L., Koga, R. (The Aerospace Corp.), and Smith, E. C. (TRW)

13a. TYPE OF REPORT	13b. TIME COVERED FROM _____ TO _____	14. DATE OF REPORT (Year, Month, Day) 1988 June 20	15. PAGE COUNT 25

16. SUPPLEMENTARY NOTATION

17.	COSATI CODES		18 SUBJECT TERMS (Continue on reverse if necessary and identify by block number)
FIELD	GROUP	SUB-GROUP	SEU Susceptibility
			Leasat Satellites
			93L422 RAMs

19. ABSTRACT (Continue on reverse if necessary and identify by block number)

In an experiment aboard three Hughes Corporation Leasat vehicles at geosynchronous orbit, single event upsets (SEU) have been continuously monitored in a memory consisting of 93L422 RAMs. Using simultaneous measurements of the high energy galactic cosmic ray and solar flare particle environment from the University of Chicago experiment aboard the IMP-8 satellite, together with a Leasat mass distribution model and ground test measurements of the SEU susceptibility for the 93L422, accurate estimates of the SEU rate are calculated based on several improvements to the standard methods. These results are discussed and compared to the Leasat flight observations.

20. DISTRIBUTION/AVAILABILITY OF ABSTRACT ☒ UNCLASSIFIED/UNLIMITED ☐ SAME AS RPT. ☐ DTIC USERS	21. ABSTRACT SECURITY CLASSIFICATION Unclassified	
22a. NAME OF RESPONSIBLE INDIVIDUAL	22b. TELEPHONE (Include Area Code)	22c OFFICE SYMBOL

DD FORM 1473, 84 MAR

83 APR edition may be used until exhausted.
All other editions are obsolete.

PREFACE

DTIC
COPY
INSPECTED

Accession For		
NTIS GRA&I	✓	
DTIC TAB	☐	
Unannounced	☐	
Justification		
By		
Distribution/		
Availability Codes		
	Avail and/or	
Dist	Special	
A-1		

1

CONTENTS

FIGURES

TABLES

I. INTRODUCTION

Since the initial suggestion that galactic cosmic rays may produce bit
errors (single-event upsets, SEU) in microelectronic devices (Ref. 1),
significant progress has been made developing techniques and methods to
estimate the rate at which such errors may be expected to occur. Upset rate
calculations depend both on the results of ground-based tests of device
susceptibility and on estimates of the high energy (galactic cosmic ray and
solar flare) particle flux to which the devices may be exposed. To date there
have been only a few opportunities to verify these methods (Ref. 2). In this
report we will present the results of one such study.

Accurate measurements of SEU rate are obtained from a reserved section of
memory in the attitude control electronics (ACE) unit aboard three Hughes
Leasat vehicles. These data are compared with calculations of the expected
upset rate based on simultaneous measurements of the high energy particle
flux, a model of the Leasat mass distribution, and ground test measurements of
SEU susceptibility. The purpose of this work is to test the methods used for
SEU rate estimation and to explore some of the major sources of error and
uncertainty inherent in those methods. This is the first time that on-orbit
measurements of SEU rates have been compared with accurate upset rate
estimates based on simultaneous measurements of the high-energy, heavy-ion
environment in which the sensitive devices were flown.

II. INPUT DATA AND ON-ORBIT OBSERVATIONS

A. LEASAT UPSET RATE MEASUREMENTS

Single-event upsets have been continuously monitored on a weekly basis aboard three Hughes Leasat vehicles (F1, F2, and F3) at geosynchronous orbit since the launch of the first satellite in late 1984. The attitude control electronics unit of each vehicle contains two 1K x 8 bit data memories made up of 93L422 bipolar RAM devices. No hamming code protection is provided for the RAM. This memory is divided into 4 pages of 8-bit memory. Pages 0, 1, and 2 (6144 bits) are used exclusively for SEU monitoring together with another 488 bits in page 3. Thus a total of 6632 bits in each memory, 13264 bits on each vehicle, are monitored regularly for SEU occurrences. The SEU activity observed during subtransfer orbits, when the vehicle passed through the energetic proton radiation zone, is not included here. Only data taken at geosynchronous orbit are used.

The number of upsets observed on each vehicle is presented in Fig. 1 for (only F1 and F2 plotted quarterly) intervals from January 1985 to September 1986. Over the whole period for which data are currently available, 775 upsets were observed on F1 in 462 days, 1608 were observed on F2 in 497 days, and 835 were observed on F3 in 232 days, yielding an average upset rate of $(1.26 \pm 0.05) \times 10^{-4}$ upsets per bit per day for F1, $(2.44 \pm 0.06) \times 10^{-4}$ upsets per bit day for F2, and $(2.71 \pm 0.09) \times 10^{-4}$ upsets per bit per day for F3. During the period when data were available from F3 (January to September 1986), the F1 and F2 upset rates were $(1.38 \pm 0.07) \times 10^{-4}$ and $(2.59 \pm 0.09) \times 10^{-4}$. The upset rates observed on F2 and F3 differ by only slightly more than one standard deviation and are statistically indistinguishable, while the rate observed on F1 is roughly half as large. Examination of the temperature profiles over the monitoring period shows that this cannot be due to a temperature effect. This phenomenon will be discussed later in this report.
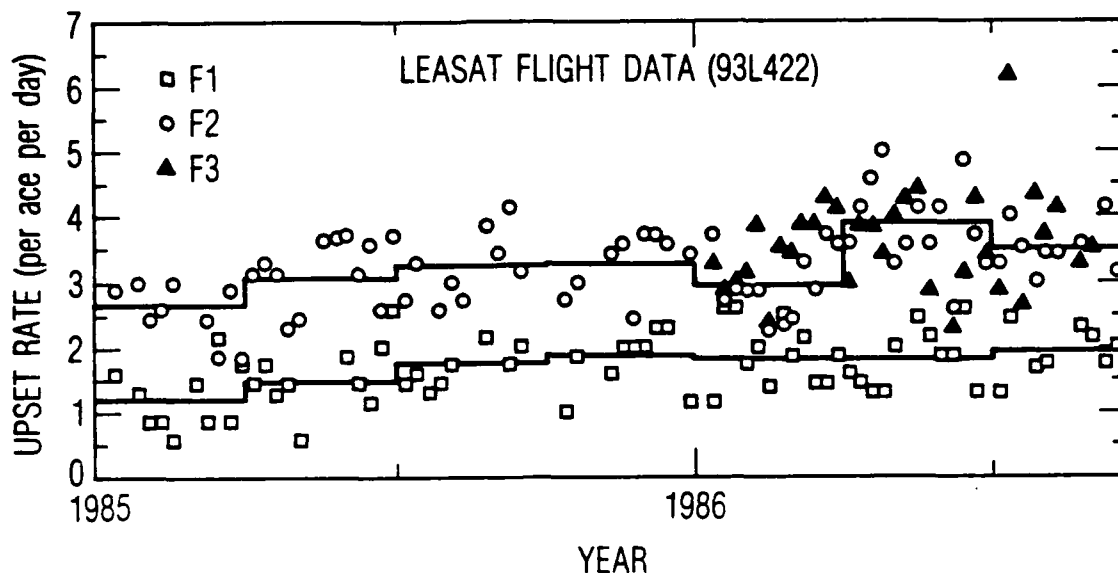
9

Fig. 1. Weekly Averages of SEU Rates Observed Aboard Leasat Vehicles

B. PARTICLE FLUX MEASUREMENTS

During the period when these Leasat data were taken, the University of
Chicago charged particle telescope aboard the satellite IMP-8 provided contin-
uous measurements of the fluxes of high-energy galactic cosmic rays and solar
flare particles. A sample of the data from this instrument is presented in
Fig. 2 (Ref. 3). These data cover an energy range comparable to the minimum
energy particles capable of penetrating the Leasat shielding to reach the
subject RAMs. Figure 2 displays the flux of helium ions in two energy ranges
(42 to 70 MeV/nucleon and 70 to 95 MeV/nucleon) and the total flux of carbon
(45 to 177 MeV/nucleon), nitrogen (49 to 184 MeV/nucleon), and oxygen (53 to
211 MeV/nucleon) ions. (We refer to this measurement as the 50 to 200 MeV/
nucleon CNO flux.) These measurements cover the period shown in Fig. 1. As
Fig. 1 illustrates, this study was conducted during a period when the galactic
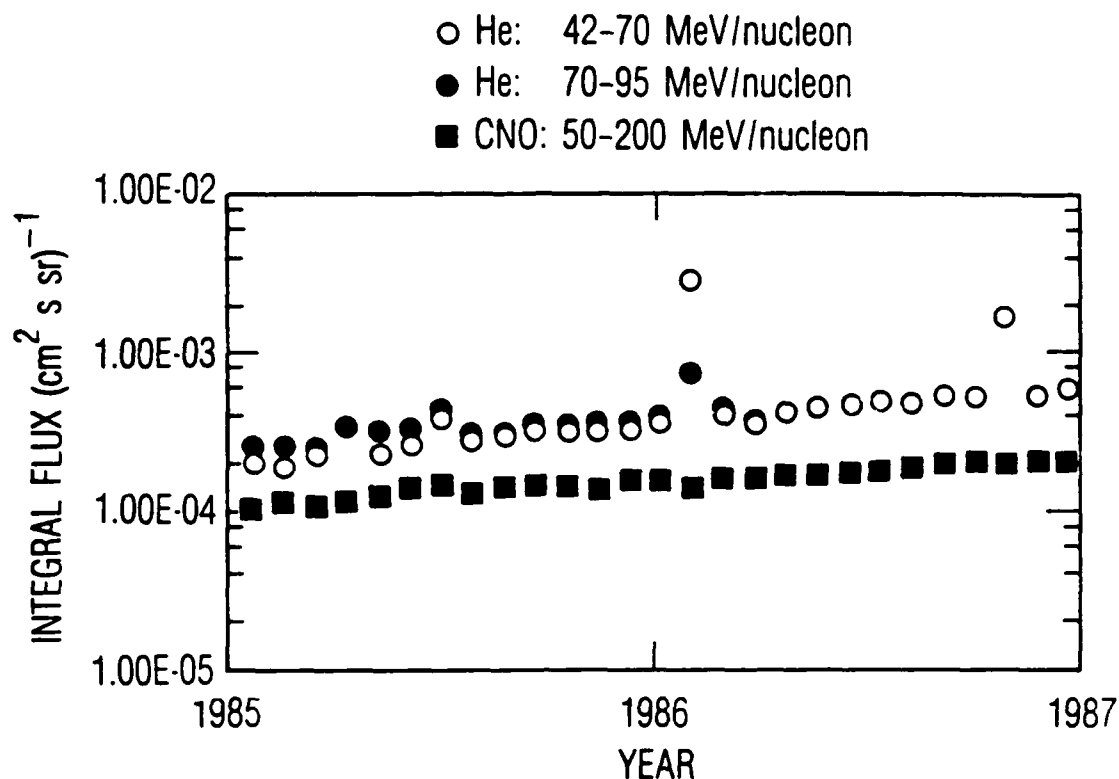
10

Fig. 2. Particle Data as Measured with the University of
Chicago Cosmic Ray Telescope Aboard Earth-Orbiting
Satellite IMP-8

cosmic ray flux was recovering from the lower intensities of the maximum in
the solar activity cycle to the higher intensities characteristic of solar
minimum expected in 1986 to 1987. This increase correlates with the gradual
increase in SEU rate observed in F1 and F2 during 1985. Two significant, but
moderate, solar flare flux increases were observed during the period when
Leasat SEUs were being monitored. These occurred in July 1985 and January
1986. The large event in November 1986 occurred after the end of the Leasat
data set available for this study.

A major goal of the present study is to determine whether and how well
these particle environment data can be used together with ground test data of
SEU susceptibility to estimate the SEU rates observed aboard Leasat.

C.   GROUND TEST DATA FOR 93L422 RAM

The 93L422 is a bipolar static RAM organized in a 256 × 4 bit configura-
tion. This device has been tested for SEU susceptibility by several groups

11

including The Aerospace Corporation (1984 to 1987), the Jet Propulsion
Laboratory (1984), and Boeing Aircraft Company (1986). These tests have shown
that the device is sensitive to SEU by relatively low linear energy transfer
(LET) ions, including carbon and oxygen, near their maximum LET. Helium ions
near end-of-range (maximum LET) may be able to upset this device, but only
with a small efficiency, and then only for long pathlengths through the
sensitive region. Ground-based tests have also demonstrated a significant
variation in 93L422 SEU susceptibility for devices from different
manufacturers.

For the upset rate calculations described in this report, ground test
data were obtained for 93L422 RAMS from two vendors, Fairchild and AMD. These
tests were run at the Lawrence Berkeley Laboratory (LBL) 88 in. cyclotron in
May 1987 by The Aerospace Corporation. The tested devices were obtained from
a collection of flight qualified parts with the same date code as those
installed in the Leasat ACE. The test devices were exposed to a variety of
ions at various energies and angles of incidence to characterize the SEU cross
section as completely as practical, using the techniques pioneered and
developed by The Aerospace Corporation gioup (Ref. 4).

The results of these tests are displayed in Fig. 3 as the SEU cross
section as a function of the "effective LET" of the incident ion. Effective
LET is the incident ion's LET divided by the cosine of the angle of incidence
of the ion from normal to the face of the device (Ref. 5). For devices in
which the volume sensitive to upset is thinnest in the direction normal to the
chip face, this effective LET provides a good measure of the "critical charge"
parameter in SEU susceptibility. It can be used in ways that minimize the
effects of unknowns in the geometry of the sensitive region (see below). Of
course, it is not the LET of the incident particle but the total charge or
energy deposited in the sensitive region that is the physical parameter
believed important to determining whether or not an upset may occur. This
belief is supported by the fact that the cosine renormalization of LET to
"effective LET" organizes the test results very well.
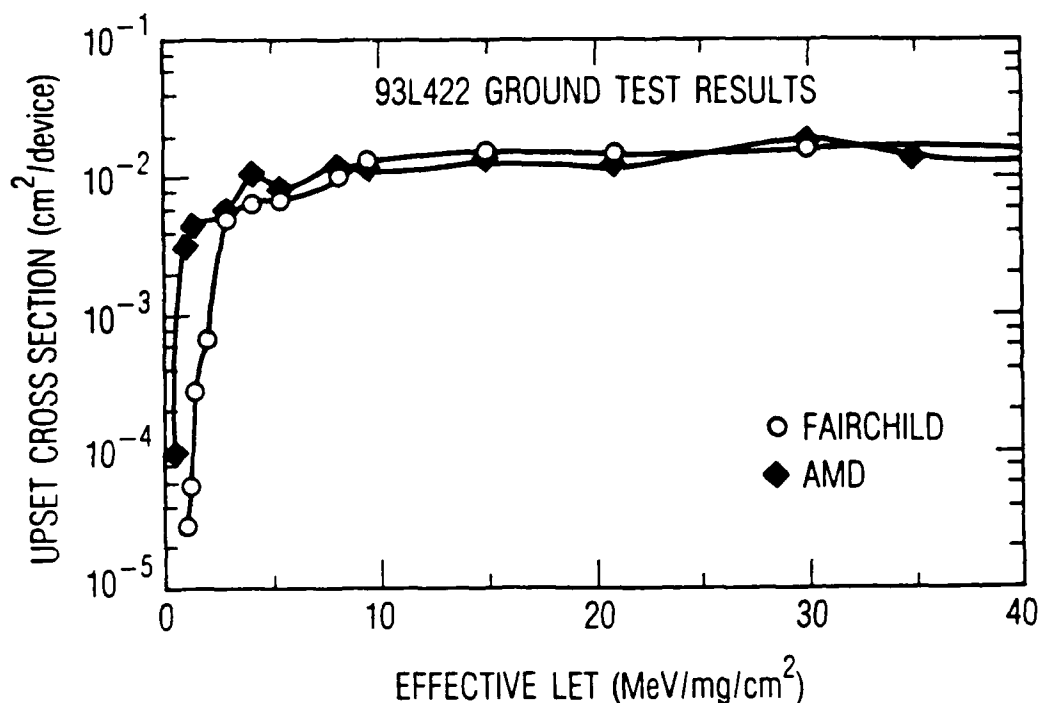
Fig. 3. Single Event Upset Cross Sections Measured by The
        Aerospace Corporation at LBL 88 in. Cyclotron in May 1987
        for 93L422 RAMs from Two Vendors: Fairchild and AMD

Figure 3 illustrates that the asymptotic SEU cross section of the
Fairchild and AMD devices is similar, but that these devices differ signifi-
cantly in the value of the LET threshold. The SEU cross section of the AMD
device is higher at lower values of the effective LET. On this basis, the AMD
device is expected to have a larger SEU rate on-orbit. (The cross section
plotted for the AMD device at the lowest LET value is not a measurement, but
an extrapolation of the measured data. This point was defined by requiring
the shape of the upset cross section for the AMD device to be the same as that
for the Fairchild device.)

13

III. METHOD FOR SEU RATE ESTIMATION

A. LET SPECTRUM CALCULATION

As Pickel and Blandford have discussed (Ref. 6), upset rate estimates may
be obtained by integrating the SEU cross section over the LET spectrum and the
geometrical distribution of pathlengths through the sensitive region. The LET
spectrum is derived from the particle flux radiation environment and the
amount of shielding surrounding the sensitive region.

Particle flux measurements from the University of Chicago's cosmic ray
instrument on the IMP-8 satellite have been used to determine the parameters
of a model for the galactic cosmic ray and solar particle energy spectrum.
The model thus constructed describes the actual environment in which the
Leasat experiment was conducted, to the extent that it may be determined from
the available particle data, and smoothly connects to standard models of the
galactic cosmic ray energy spectrum at energies above the maximum particle
energy detected by the IMP-8 experiment. The particle flux intensity during
the period of interest was increasing smoothly as the galactic cosmic ray
intensity continued its recovery from solar maximum toward solar minimum (see
Fig. 2). Because these changes were not large, and in order to obtain better
statistical precision from the IMP-8 measurements, we limited the comparison
to two 6-month periods at each end of the Leasat data interval: the first
half of 1985, and April to September 1986. These periods were also chosen
because they are free of any significant increases due to solar flares.

For the present study, we have based our particle environment model on
the model provided by Adams in his CREME code (Ref. 7), and used the cosmic
ray data displayed in Fig. 2 to constrain parameters of Adam's model. To
begin, we removed the components in the model which describe the cosmic ray
anomalous component, and any interplanetary or solar contributions, to concen-
trate on the solar cycle effect. We determined values for a parameter, s,
which describes the amount of mixing between Adam's solar minimum (f_{min}) and
solar maximum (f_{max}) galactic cosmic ray spectra by requiring the resulting
model:

$$f(s) = (1 - s) f_{min} + s f_{max}$$

to yield the observed value of the 50 to 200 MeV/nucleon CNO flux. For the 1985 period, s = 0.60, while s = 0.25 for the 1986 interval. We believe that this model provides a good description of the high energy flux for the galactic cosmic ray component. However, if these results are then used to predict the helium flux measurements displayed in Fig. 2, they give a lower flux than observed. This deviation provides a good measure of the amount of the "anomalous component" of helium that must be added back into our model.

The form for the anomalous helium component which we added was motivated by the observations of Garcia-Munoz, et al. (Ref. 8). They demonstrate an enhancement over the nominal galactic cosmic ray the helium spectrum below ~100 MeV/ nucleon which increases with decreasing energy. To model this, we adopted a simple helium enhancement factor (F) to multiply Adams's model for helium with energies (E) between 10 and 100 MeV/nucleon of the form:

$$F = A^{((100-E)/90)}$$

Thus A is the enhancement factor at 10 MeV/nucleon. We found that both helium flux-energy range measurements could be fit to better than 5 percent (less than the statistical precision of the measurements) by adopting A = 1.22 for the 1985 period, and A = 1.65 for the period in 1986.

B. LEASAT SHIELDING DISTRIBUTION

In order to calculate the LET spectrum at the sensitive device from the particle environment model, the distribution of shielding material around the device must be known. An accurate model of the Leasat spacecraft was available and used together with a sector ray-tracing code to determine this shielding distribution, which is shown in Fig. 4.

For each of the two periods, a LET spectrum was calculated at each value of shielding thickness tabulated in the sector code output. The resulting spectra were summed, each weighted by the fraction of solid angle given by the ray-tracing results. The result of this calculation thus was an average LET spectrum properly weighted by the actual Leasat mass shielding distribution. The LET spectra for the 1985 and 1986 periods which resulted from these calculations are displayed in Fig. 5.
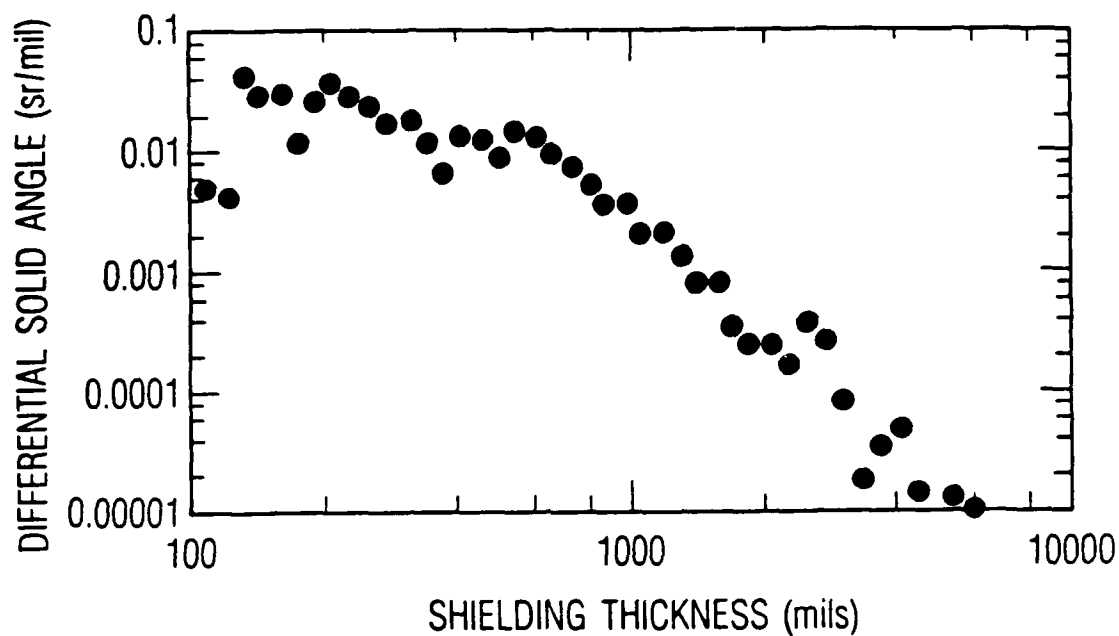
Fig. 4. Shielding Distribution on Leasat Vehicle Surrounding
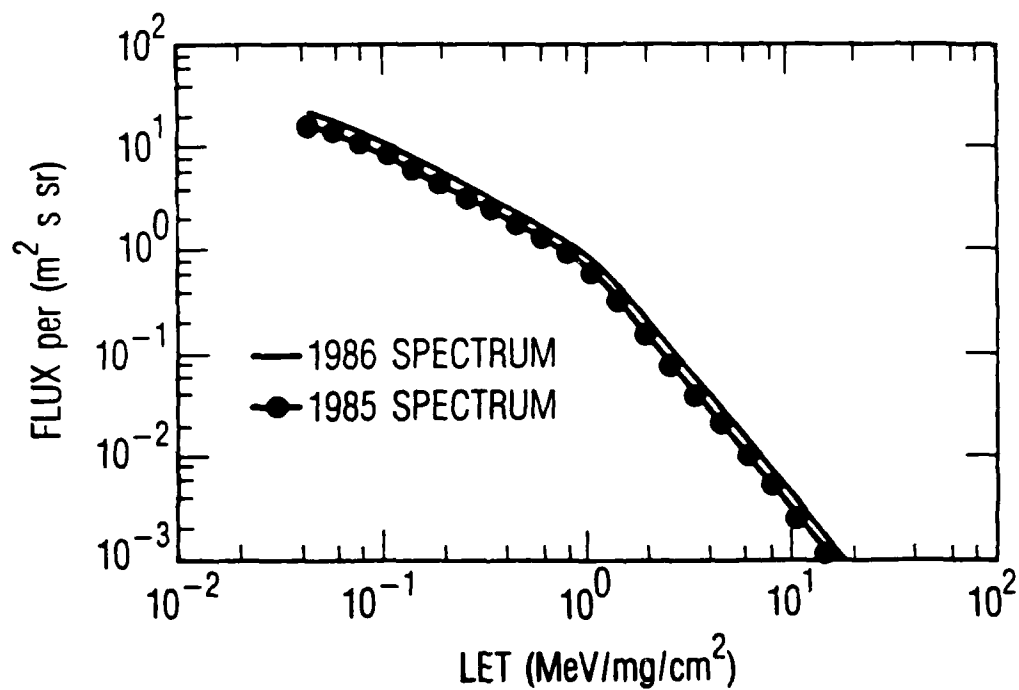Memory in Attitude Control Electronics Computer

Fig. 5. Calculated LET Spectra Based on Heavy Ion Environment Model
and Leasat Shielding Distribution for Two Periods (Early 1985
and Mid-1986)

17

C. SEU RATE CALCULATION METHOD

It is customary to express the device upset cross section as a step function with a value equal to the measured asymptotic value for all values of deposited charge (Q) above a critical charge threshold, $(Q > Q_c)$ (Ref. 6). Given this approximation, the SEU rate can be calculated as a single integral of the product of the integral LET spectrum F(L) and the distribution of pathlengths through the sensitive region of the device, p(l) dl. The range of integration covers all pathlengths, l, from zero to the maximum pathlength possible through the sensitive volume, but this range is limited by the re-quirement that the product of the LET (L) and the pathlength, l, must exceed the critical charge threshold $(L\ l > Q_c)$. Petersen et al. (Ref. 9) have discussed the errors inherent in this method for devices with measured cross sections that are not well described by the step function approximation.

For this study, we have developed a method which removes the step function approximation by explicit integration over the shape of the measured cross section. In our method, we normalize the pathlength distribution such that p(l) dl is the differential solid angle, area product of the sensitive region for pathlength l. We have assumed that the sensitive region can be approximated as a right rectangular prism with area A = d x w and thickness t, and have adopted an expression similar to that given by Pickel and Blandford (Ref. 6) for the pathlength distribution, but with a different normalization.

The values chosen for the dimensions of the region (d, w, t) are deter-mined from the experimental SEU cross section measurements as a function of effective LET, $\sigma(L^*)$. We assume that for each bit there is a single sensitive volume. The asymptotic SEU cross section per bit at large L^* is identified with the sensitive area, A = (d w). A value for the thickness, t, is assumed and used to convert the effective LET to deposited charge, $Q = t\ L^*$. Since the geometry of the sensitive region is described by the pathlength distribu-tion, the measured cross section is renormalized so that it functions as an efficiency factor:

$$\epsilon(Q) = \sigma(Q)/A$$

18

Conceptually, $\epsilon(Q)$ describes the probability that a charge deposit Q in the sensitive volume will cause an upset. Finally in our method, the integral LET spectrum calculated by the method described above is differentiated to obtain f(L) dL as the particle flux per unit area, solid angle, and time in the LET interval dL. With these definitions, the SEU rate (R) is calculated as the double integral:

$$R = \iint [\epsilon(Q = 1L) \; f(L) \; p(1)] \; d1 \; dL$$

The range of both integrals is over the region from 0 to the maximum possible pathlength or LET. We performed this calculation by repeated gaussian numerical integration on a mesh. The integration was rerun, each time doubling the number of mesh points, until consistent results were obtained with an estimated ultimate numerical accuracy of better than 1 percent.

The real advantage of this method is that it removes the ad hoc assumption of a form for the upset cross section. Of course, it is possible to use the step function approximation and to assume a LET threshold based on experience or intuition. Some selection of LET threshold will yield the same value of the SEU rate as the more rigorous double integral method, but the selection of that threshold will depend on the shapes both of the upset cross section and the LET spectrum in a way which may be difficult to determine.

IV. DISCUSSION

A. NUMERICAL RESULTS

There are three features of our method which deserve consideration before we compare the numerical results to the flight data. They are: 1) how to handle the uncertainties in the measured cross section; 2) the selection of a value for the thickness of the sensitive volume (t); and 3) the choice of aspect ratio, i.e., specific values for the dimensions w and d in the path-length distribution when only their product (A) is determined.

Uncertainties in the measured cross section are a potential source for significant errors, both systematic and random. We cannot address the systematic errors here. The random errors result from a variety of sources, e.g., counting statistics, beam nonuniformity, and chip orientation in the beam. The consistency of cross section values in the asymptotic region provides one measure of the magnitude of these errors. In our numerical integrations we have applied the measured cross section results in three ways, each involving a different choice for the cross section between measured values. The choices made were: 1) the lower of the neighboring points; 2) the upper of the neighboring points; and 3) linear interpolation between neighboring points. The first and second of these methods lead to significant under- and over-estimates of the expected SEU rate, while the last method lies in between.

Table 1 shows that the SEU rates calculated from the upper and lower limits differ by a factor of 2 to 3. While this range represents a significant overestimate of the effects of cross section uncertainties on our results, it is also, by far, the largest source of uncertainty in our calculation. Numerical errors are estimated at less than a few percent, and random, statistical, uncertainties in the measured environment probably contribute less than 10 percent to the uncertainty in the calculated rate. This conclusion is based on a comparison of the differences between the SEU rate calculations for the 1985 and 1986 periods. Thus we firmly believe that the real uncertainties in our numerical results are well within the ranges quoted in Table 1, and we have adopted the result of the linear interpolation method as our best value for the calculated upset rate.

21

Table 1. 93L422 SEU Rate-Results for Various
Assumed Thicknesses and Flight Data

| Vendor	Thickness, μm	Calculated SEU Rate* (Upsets per Chip per Day)	
		1985 Nominal (Range)	1986 Nominal (Range)
Fairchild	1	0.196 (0.144, 0.293)	0.253 (0.186, 0.383)
Fairchild	2	0.189 (0.138, 0.287)	0.243 (0.178, 0.377)
Fairchild	4	0.177 (0.129, 0.281)	0.230 (0.167, 0.369)
Fairchild	8	0.161 (0.113, 0.269)	0.207 (0.146, 0.353)
AMD	1	0.598 (0.404, 0.942)	0.760 (0.520, 1.250)
AMD	2	0.589 (0.398, 0.949)	0.758 (0.512, 1.268)
AMD	4	0.582 (0.390, 0.950)	0.744 (0.501, 1.269)
AMD	8	0.561 (0.376, 0.975)	0.723 (0.480, 1.293)
Observed On-orbit		1985	1986
F1		0.101 ± 0.008	0.142 ± 0.009
F2		0.222 ± 0.011	0.288 ± 0.012
F3		N/A	0.286 ± 0.012

*1985 refers to the period January through June 1985. 1986 refers to the period April to
September 1986. The "Nominal" value was calculated by linear interpolation of the
experimental SEU cross-section. The limits of the "Range" were calculated from the
lower and upper limits of the measured cross-section (see text). Quoted uncertainties in
the observed error rates are 1 sigma for the statistical error of the measurement.

Due to the nature of the ground-based SEU tests, the assumption of a
thickness for the sensitive region had only a second order effect on our
calculation. This is because ground-based tests determine the cross section
as a function of "effective LET," not deposited (or collected) charge in the
sensitive region. It is possible to estimate a likely value for the
thickness, and for the 93L422 we estimated a value of 2 μm. We have investi-
gated the effect of this assumption, as shown in Tables 1 and 2 and in Fig.
6a, and found that the calculated upset rate for an assumed thickness of
8 μm was within 15 percent of the value calculated for the 2 μm case.

Figure 6b and Table 2 show the results obtained under various assumptions
of the values for w and d, the other dimensions of the sensitive region. In
all of these cases the product (w d), which is the area of the device parallel
to the chip face, was fixed at 1521 μm^2, while t was fixed at 2 μm. For an
aspect ratio of 1, the sensitive volume is a slice of a cube, 39 μm on a side
by 2 μm thick. For an aspect ratio of 64, the sensitive volume has dimensions
4.875 x 312 x 2 μm. The total variation in the calculated upset rate over
this range was less than 6 percent.

22
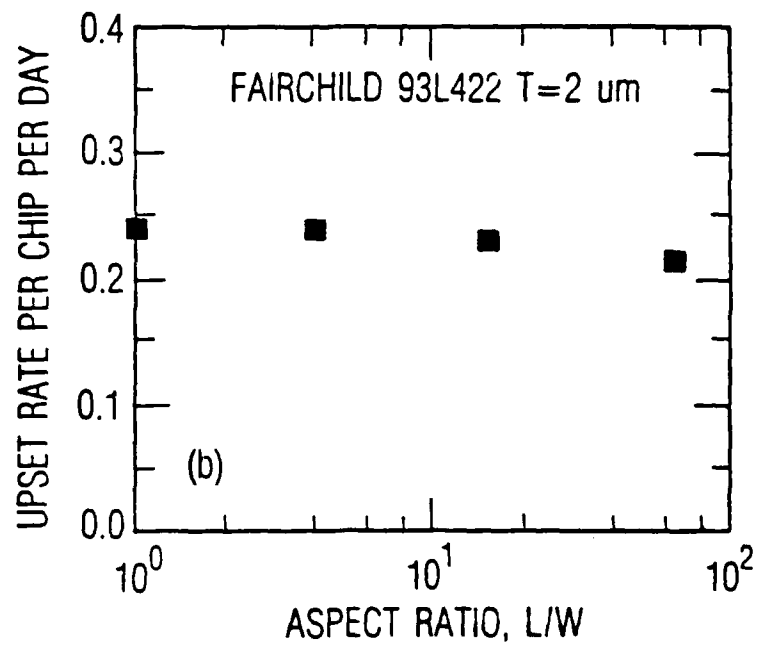
a) Assumed thickness for Sensitive Region of
   Fairchild Device
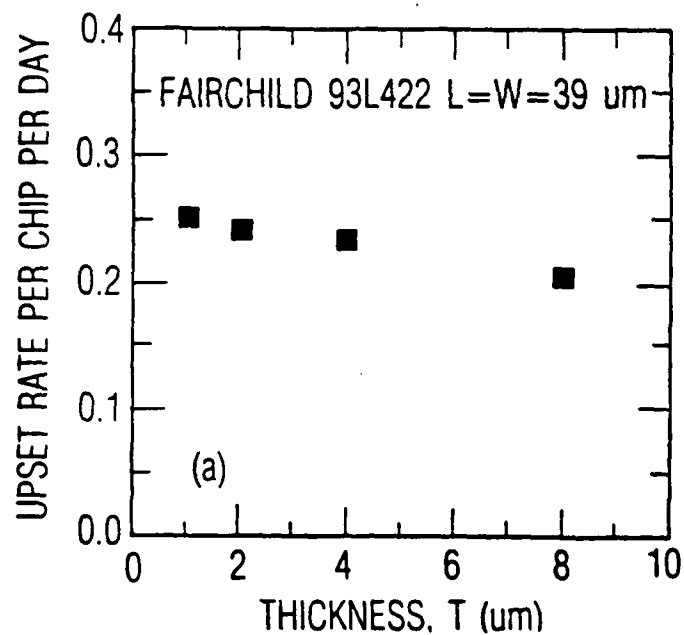
b) Assumed Aspect Ratio for Area of Sensitive
   Region Parallel to Chip Face

Fig. 6. Calculated SEU Rate

23

Table 2. 93L422 SEU Rate Variation
with Sensitive Region Size
for Fairchild Device

Sensitive Region Dimensions, μm			Calculated Upset Rate (1986 Spectrum), Per Chip Per Day
W	D	T	
39	39	1	0.253
39	39	8	0.207
39	39	2	0.243
78	19.5	2	0.242
156	9.75	2	0.233
312	4.875	2	0.217

Table 1 also shows that the SEU rate calculated for the AMD device is just over three times the rate calculated for the Fairchild device. This difference is in the direction expected on the basis of the differences in cross section at low values of LET. Comparing the rates calculated for the 1985 period with those calculated for 1986 indicates an increase of 29 percent. This difference is due solely to the effects of the changes in the cosmic-ray environment.

B. COMPARISON OF NUMERICAL RESULTS TO FLIGHT DATA

Table 1 also shows the upset rates observed on-orbit for each of the two periods for each vehicle. The upset rates observed on F2 and F3 are well within the ranges calculated for the Fairchild devices. Compared to the preferred "linear interpolation" value, the observed rates are about 18 percent higher. This difference is nearly 3 standard deviations of the observed F2 and F3 rates, but, as discussed above, it is probably within the reasonable range of uncertainty of the calculated rate.

None of the calculated cases is close to the upset rates observed on F1, which are almost exactly half of the rates observed on F2 and F3. Before these calculations were completed, it was hoped that the difference between the F1 versus F2 and F3 upset rates may be explained by the differences between the upset cross sections of the Fairchild and AMD devices. However, since the

24

calculated rate for the AMD devices is 2 to 3 times higher than even the F2 and F3 rates, then, if we accept these calculations, we must conclude that no AMD devices were used in the F2 and F3 memories, and we must search for another explanation for the F1 versus F2 and F3 difference. The fact that the difference between F1 and F2 or F3 is almost exactly a factor of 2 suggests a possibility that we will continue to explore, namely, that the F1 upsets have been monitored in only one of the two ACE memories.

One way to minimize the effects of some kinds on our analysis of systematic errors is to compare the differences between the two time periods. The increase in upset rate observed in the 1986 period compared to the 1985 period is 40 ±14 percent for F1 and 30 ±8 percent for F2. The increase in the calculated upset rate is in the range 27 to 34 percent for all cases, and, based on the calculations for the Fairchild device, a preferred value of 29 percent is inferred. This good agreement between the calculation and the observations is an important confirmation of the quality of the environment model and the other factors and methods that contribute to the calculation of the LET spectra used here, including the shielding model.

C. SOLAR FLARE EFFECTS

Finally, we noted that there were two moderate solar flares during the period covered by these Leasat upset rate observations. Increases in the helium ion flux due to these flares are readily apparent in Fig. 2, but increases in the 50 to 200 MeV/nucleon CNO flux are difficult to discern there. Thus, we must conclude that due to differences in the composition and energy spectra between the flare ions and the galactic cosmic rays, the contribution to the total CNO flux due to these flares is almost negligible. Since in the energy interval from 10 to 300 MeV/nucleon the typical ion energy spectrum from flares decreases with increasing energy while the galactic cosmic ray flux increases with increasing energy, these flares are probably even less important at higher energies than the CNO flux of Fig. 2 suggests. From this perspective, therefore, since only energetic ions heavier than helium are efficient producers of SEU in the Leasat memories, it is not surprising that there is no observable increase in the measured upset rate during these flares.

25

V. SUMMARY AND CONCLUSIONS

Measurements of on-orbit SEU rates in the 93L422 bipolar RAM have been obtained during 1985 and 1986 aboard the Hughes Leasat vehicles. To interpret these results, we have used simultaneous measurements of the energetic heavy ion flux obtained by the University of Chicago cosmic ray telescope aboard the IMP-8 satellite, an accurate model of the Leasat mass distribution, comprehensive ground-test characterization of the device upset cross section, and methods to calculate SEU rates which incorporate several improvements over the standard techniques. We found that the calculated results agreed with the on-orbit SEU rates for two of the Leasat vehicles to within 20 percent, assuming that the flight memories were fabricated from Fairchild devices. We believe that this 20 percent difference is within the range of uncertainty inherent in the calculation. The largest contribution to the uncertainty of the calculation is due to uncertainties in the ground-based characterization of the upset cross section.

The method of calculation and the calculated results were analyzed to show the effects of various assumptions concerning the geometry of the sensitive region. All such effects and assumptions were shown to be small, in the range of 5 to 15 percent of the recalculated SEU rate.

Differences in the observed upset rates during two separate periods of the study were 30 to 40 percent, consistent with the calculated values to within the uncertainty of the measurement. These differences are the result of changes in the cosmic ray environment due to changes in the level of solar modulation of the galactic cosmic ray flux. This provides important confirmation of the accuracy of the environment model and the methods of calculation.

The upset rate observed on one of the Leasat vehicles (F1) was only half of that observed on the other two (F2 and F3). We cannot yet explain this difference.

27

REFERENCES

1. D. Biner, E. C. Smith, and A. B. Holman, IEEE Trans. Nuc. Sci., NS-22, 2675 (December 1975).

2. For example, see J. B. Blake and R. Mandel, IEEE Trans. Nuc. Sci., NS-33, 1616 (December 1986).

3. K. R. Pyle, private communication (1987).

4. R. Koga, W. A. Kolasinski, and S. Imamoto, IEEE Trans. Nuc. Sci., NS-32, 159 (December 1985).

5. R. Koga, W. A. Kolasinski, IEEE Trans. Nuc. Sci., NS-31, 1190 (December 1984).

6. J. C. Pickel and J. T. Blandford, IEEE Trans. Nuc. Sci., NS-27, 1006 (April 1980).

7. J. H. Adams, Jr., R. Silberberg, and C. H. Tsao, "Cosmic Ray Effects on Microelectronics, Part 1: The Near-Earth Particle Environment," NRL Memorandum Report 4506 (25 August 1981, and updates thereto).

8. M. Garcia-Munoz, K. R. Pyle, and J. A. Simpson, "The Anomalous Helium Components in the Helisphere: The 1 AU Spectra During the Recovery from the 1981 Solar Maximum," in contributions to the 20th International Cosmic Ray Conference, paper SH 6.4-11 (1987).

9. E. L. Petersen, J. B. Langworthy, and S. E. Diehl, IEEE Trans. Nuc. Sci., NS-30 (December 1983).

REFERENCES

1. D. Biner, E. C. Smith, and A. B. Holman, _IEEE Trans. Nuc. Sci._, _NS-22_, 2675 (December 1975).

2. For example, see J. B. Blake and R. Mandel, _IEEE Trans. Nuc. Sci._, _NS-33_, 1616 (December 1986).

3. K. R. Pyle, private communication (1987).

4. R. Koga, W. A. Kolasinski, and S. Imamoto, _IEEE Trans. Nuc. Sci._, _NS-32_, 159 (December 1985).

5. R. Koga, W. A. Kolasinski, _IEEE Trans. Nuc. Sci._, _NS-31_, 1190 (December 1984).

6. J. C. Pickel and J. T. Blandford, _IEEE Trans. Nuc. Sci._, _NS-27_, 1006 (April 1980).

7. J. H. Adams, Jr., R. Silberberg, and C. H. Tsao, "Cosmic Ray Effects on Microelectronics, Part 1: The Near-Earth Particle Environment," NRL Memorandum Report 4506 (25 August 1981, and updates thereto).

8. M. Garcia-Munoz, K. R. Pyle, and J. A. Simpson, "The Anomalous Helium Components in the Helisphere: The 1 AU Spectra During the Recovery from the 1981 Solar Maximum," in contributions to the 20th International Cosmic Ray Conference, paper SH 6.4-11 (1987).

9. E. L. Petersen, J. B. Langworthy, and S. E. Diehl, _IEEE Trans. Nuc. Sci._, _NS-30_ (December 1983).

LABORATORY OPERATIONS

The Aerospace Corporation functions as an "architect-engineer" for national security projects, specializing in advanced military space systems. Providing research support, the corporation's Laboratory Operations conducts experimental and theoretical investigations that focus on the application of scientific and technical advances to such systems. Vital to the success of these investigations is the technical staff's wide-ranging expertise and its ability to stay current with new developments. This expertise is enhanced by a research program aimed at dealing with the many problems associated with rapidly evolving space systems. Contributing their capabilities to the research effort are these individual laboratories:

Aerophysics Laboratory: Launch vehicle and reentry fluid mechanics, heat transfer and flight dynamics; chemical and electric propulsion, propellant chemistry, chemical dynamics, environmental chemistry, trace detection; spacecraft structural mechanics, contamination, thermal and structural control; high temperature thermomechanics, gas kinetics and radiation; cw and pulsed chemical and excimer laser development including chemical kinetics, spectroscopy, optical resonators, beam control, atmospheric propagation, laser effects and countermeasures.

Chemistry and Physics Laboratory: Atmospheric chemical reactions, atmospheric optics, light scattering, state-specific chemical reactions and radiative signatures of missile plumes, sensor out-of-field-of-view rejection, applied laser spectroscopy, laser chemistry, laser optoelectronics, solar cell physics, battery electrochemistry, space vacuum and radiation effects on materials, lubrication and surface phenomena, thermionic emission, photo-sensitive materials and detectors, atomic frequency standards, and environmental chemistry.

Computer Science Laboratory: Program verification, program translation, performance-sensitive system design, distributed architectures for spaceborne computers, fault-tolerant computer systems, artificial intelligence, micro-electronics applications, communication protocols, and computer security.

Electronics Research Laboratory: Microelectronics, solid-state device physics, compound semiconductors, radiation hardening; electro-optics, quantum electronics, solid-state lasers, optical propagation and communications; microwave semiconductor devices, microwave/millimeter wave measurements, diagnostics and radiometry, microwave/millimeter wave thermionic devices; atomic time and frequency standards; antennas, rf systems, electromagnetic propagation phenomena, space communication systems.

Materials Sciences Laboratory: Development of new materials: metals, alloys, ceramics, polymers and their composites, and new forms of carbon; non-destructive evaluation, component failure analysis and reliability; fracture mechanics and stress corrosion; analysis and evaluation of materials at cryogenic and elevated temperatures as well as in space and enemy-induced environments.

Space Sciences Laboratory: Magnetospheric, auroral and cosmic ray physics, wave-particle interactions, magnetospheric plasma waves; atmospheric and ionospheric physics, density and composition of the upper atmosphere, remote sensing using atmospheric radiation; solar physics, infrared astronomy, infrared signature analysis; effects of solar activity, magnetic storms and nuclear explosions on the earth's atmosphere, ionosphere and magnetosphere; effects of electromagnetic and particulate radiations on space systems; space instrumentation.

. . .